Amino Acids (2012) 42:2149–2163
DOI 10.1007/s00726-011-0953-8

ORIGINAL ARTICLE

Identification of c-myc-dependent proteins in the medulloblastoma cell line D425Med

Amedeo A. Azizi · Lin Li · Thomas Ströbel · Wei-Qiang Chen · Irene Slavc · Gert Lubec

Received: 25 May 2011 / Accepted: 26 May 2011 / Published online: 12 June 2011

Abstract High c-myc levels are linked to poor prognosis in medulloblastoma (MB), and it was the aim of the current study to search for c-myc-dependent proteins in the MB cell line D425Med. For this purpose D425Med cells and cells with knocked-down c-myc (by siRNA) were analysed by a gel-based differential proteomics study using mass spectrometry. Heterogeneous nuclear ribonucleoproteins C1/C2, heterogeneous nuclear ribonucleoprotein A/B, stathmin, endoplasmic reticulum protein ERp29 precursor and guanidinoacetate *N*-methyltransferase were c-myc dependently expressed. Signalling, the protein machinery, metabolism and endoplasmic reticulum function may be affected and these results enable studying tumour tissue for these proteins as potential dignity markers or pharmacological targets.

Keywords Brain tumour · Medulloblastoma · c-myc · myc

Abbreviations

2DE	Two-dimensional gel electrophoresis
GAMT	Guanidinoacetate *N*-methyltransferase
hnRNP	Heterogeneous nuclear ribonucleoprotein
hTERT	Human telomerase reverse transcriptase
MB	Medulloblastoma
PNET	Primitive neuroectodermal tumour

A. A. Azizi and L. Li contributed equally to this work.

Electronic supplementary material The online version of this article (doi:10.1007/s00726-011-0953-8) contains supplementary material, which is available to authorized users.

A. A. Azizi · L. Li · W.-Q. Chen · I. Slavc · G. Lubec (✉)
Department of Pediatrics, Medical University of Vienna, Währinger Gürtel 18, 1090 Vienna, Austria
e-mail: gert.lubec@meduniwien.ac.at

T. Ströbel (✉)
Institute of Neurology, Medical University of Vienna, Währinger Gürtel 18, 1090 Vienna, Austria
e-mail: thomas.stroebel@meduniwien.ac.at

Introduction

Central nervous system (CNS) tumours constitute the largest group of solid neoplasms in childhood and are the leading cause of cancer-related death and morbidity in children (Jemal et al. 2008). The medulloblastoma (MB) is the most frequent malignant brain tumour in childhood and an invasive primitive neuroectodermal tumour of the cerebellum (MacDonald et al. 2003). MBs represent approximately 20% of all childhood brain tumours (MacDonald et al. 2003). Treatment is complicated by the tendency of approximately one-third of these tumours to disseminate throughout the CNS early in the course of disease (Packer 2008).

Current therapy includes maximum surgical resection, whole neuroaxis irradiation, and chemotherapy (MacDonald et al. 2003; Packer 2008; von Hoff et al. 2009). Treatment causes long-term morbidity including endocrine and growth disturbances, as well as neurocognitive dysfunction, which is particularly severe in young children (Chapman et al. 1995; Dennis et al. 1996; Radcliffe et al. 1992; Silber et al. 1992). Despite aggressive treatment, only 60% of children with MB will be cured (von Hoff et al. 2009). Consequently, efforts are being made to stratify patients according to their individual risk of tumour relapse or progression (Goldwein et al. 1996; Grotzer et al.

2007; Rutkowski et al. 2007; Zeltzer et al. 1999). By identifying patients who can be cured with less intensive therapy late effects of treatment could be reduced without endangering the high level of treatment efficacy. Vice versa, patients at high risk may receive more intensive therapy.

At present, children with MB are divided into two risk groups. Average-risk (AR) patients are those diagnosed when they are older than the age of 3 years with non metastatic and totally or near-totally resected ($\leq$1.5 cm^2 on postoperative magnetic resonance imaging) MB; patients not fulfilling these criteria are regarded as high risk (von Hoff et al. 2009; Zeltzer et al. 1999). Histopathological findings with differentiation of MB in different histological subgroups have recently led to the identification of a third risk group: Children with desmoplastic MB or MB with extensive nodularity show a higher overall survival than AR MB patients (Rutkowski et al. 2009). This clinical stratification has only proven useful as a broad guide for predicting prognosis; in particular, it does not identify the 20–30% of AR patients with resistant disease or the unknown number of AR patients who might be overtreated with current protocols.

The likelihood of finding additional clinical prognostic factors is small, therefore a quest for biological prognostic factors is ongoing (Das et al. 2009; Gilbertson et al. 2001; Grotzer et al. 2007; Korshunov et al. 2008; Pfister et al. 2009; Rutkowski et al. 2007).

Different biological markers have so far been associated with clinical outcome. Amongst the best described are (1) proto-oncogene MYC (c-myc) mRNA expression (2) copy number aberrations of chromosomes 17q, 6q, *c-myc* and *n-myc*, (3) ErbB2 and ErbB4 receptor expression, (4) neurotrophin receptor TrkC expression, (5) Beta-catenin mutation and nuclear accumulation and (6) p53 mutation (Das et al. 2009; Ellison et al. 2005; Fattet et al. 2009; Gilbertson et al. 2001; Grotzer et al. 2001; 2007; Herms et al. 2000; Pfister et al. 2009; Ray et al. 2004; Rogers et al. 2009; Rutkowski et al. 2007; von Hoff et al. 2010). Low c-myc mRNA expression was identified as an independent predictor of a favourable survival outcome (Grotzer et al. 2001, 2007; Herms et al. 2000). The 5-year cumulative progression-free survival was significantly higher in case of low levels of MYC mRNA expression (92% as compared to 38%). MYC mRNA expression levels did not correlate with metastatic stage, age, or gender of MB patients nor with *MYC* gene amplification. This indicates that MYC mRNA expression is of independent prognostic significance. Combination of c-myc with TrkC mRNA expression led to the identification of three risk groups: (1) low c-myc and high TrkC with a good prognosis, (2) high c-myc and low TrkC with poor prognosis and (3) the remaining patients with intermediate prognosis. These findings could be repeated in a larger cohort (Grotzer et al. 2007). *MYC* gene amplification has been suggested as an indicator of poor prognosis in two studies of 29 and 77 MB patients, respectively (Aldosari et al. 2002; Scheurlen et al. 1998).

The *c-myc* proto-oncogene encodes a nuclear phosphoprotein involved in transcription of genes central to regulating cell cycle, cellular proliferation, apoptosis, and differentiation (Henriksson and Luscher 1996; Obaya et al. 1999; Prendergast 1999; Schmidt 1999). *c-myc* expression is normally tightly regulated throughout the cell cycle, but may become deregulated or activated contributing to malignant transformation (Claassen and Hann 1999). Dysregulation of *myc* has been implicated in the pathogenesis of a variety of human neoplasms (Nesbit et al. 1999). Whilst gene amplification is an important mechanism of *MYC* dysregulation, it is uncommon in MB, with an incidence of <10% in primary tumours (Herms et al. 2000). Up-regulation of *c-myc* in MB independent of gene amplification may involve the adenomatous polyposis coli (APC) and beta-catenin (CTNNB1) pathways. A subset of MB is associated with Turcot's syndrome, which is the association of colon cancer with primary brain tumours and is characterised by germ-line mutations in the APC gene (Hamilton et al. 1995). Whilst mutations of APC have not been detected in sporadic MB, approximately 5% of sporadic MB have been reported to contain mutations in a second Wingless/Wnt pathway member, beta-catenin (Eberhart et al. 2000; Mori et al. 1994; Zurawel et al. 1998). Mutations in either APC or beta-catenin act to stabilise beta-catenin protein, which accumulates and translocates into the nucleus where it complexes with Tcf4 and up-regulates the transcription of *c-myc* as well as other targets (Bullions and Levine 1998; He et al. 1998). Aberrant nuclear beta-catenin staining has been demonstrated in 18% of sporadic MB and in one MB from a patient with Turcot's syndrome (Eberhart et al. 2000). Nevertheless, in different MB cell lines, factors other than or in addition to those mentioned were responsible for c-myc over-expression (Liu and Levens 2006; Siu et al. 2003). In contrast to colon cancer, the causative agents of *c-myc* promoter activation in MB remain to be identified.

In MB, c-myc genomic amplification and mRNA expression is also associated with particularly aggressive histological tumour subtypes (large cell/anaplastic) and poorer patient survival (Stearns et al. 2006). However, the biological basis for this correlation remains elusive.

The group of M. Grotzer studied MB cell lines DAOY, D425, and D341 exhibiting different levels of c-myc expression (von Bueren et al. 2007). Down-regulation of c-myc levels using siRNA led to inhibition of cellular proliferation and clonogenic growth, to inhibition of G1–S phase cell cycle progression and to a decrease in human telomerase reverse transcriptase (hTERT) expression and

telomerase activity. It was furthermore shown that reduction in c-myc levels reduced apoptosis and decreased the sensitivity of MB cells to irradiation and chemotherapeutic agents (von Bueren et al. 2009).

The aim of this study was the identification of differences in the protein pattern of c-myc expressing MB cells as compared to MB cells after down-regulation of c-myc by 2D-gel electrophoresis and mass spectrometric protein identification. Proteins showing increased levels in cells with abundant c-myc expression may contribute to the malignant behaviour of c-myc over-expressing MB by playing a role in the ability of these cells to proliferate, metastasise or enhance drug resistance. Conversely, proteins found to be decreased might act as tumour suppressors in non-transformed cells, e.g. enhancing the cell to undergo apoptosis, arresting cell cycle or inducing neuronal differentiation.

To the authors' knowledge, this study is the first to analyse the differential proteome depending on high and low c-myc expression.

Materials and methods

Cell culture

The human MB/PNET cell line D425Med was purchased from the American Type Culture Collection (Manassas, VA, USA). Cells were cultured at 37°C in 5% CO_2 in Dulbecco's modified Eagle's medium (DMEM) supplemented with 10% FBS, 2% L-glutamine (27 mg/ml) and 1% penicillin/streptomycin (100 IU/ml penicillin, 100 µg/ml streptomycin).

Transfection and RNAi

The *c-myc* gene was silenced using RNA inhibition (RNAi) techniques by introducing a *c-myc* gene-specific siRNA in a pSilencer® vector (Ambion, Huntington, UK).

Different siRNA sequences were tested in pilot experiments to identify the siRNA sequence that showed the highest degree of gene silencing in transient assays. To downregulate c-myc, we cloned the sequence GAGAAC TTCTACCAGCAGCTTCAAGAGAGCTGCTGGTAGA AGTTCTCCTTTTTTTGGAA into the *Bam*HI/*Hin*dIII-sites of the pSilencer 3.1 plasmid (Ambion, Huntington, UK) according to the manufacturer's instructions. As negative control, a siRNA with no sequence specificity to any human gene (Ambion) was cloned into the pSilencer 3.1 plasmid. These two plasmids were used to transfect D425Med cells using lipofection (Transfast; Promega, Wisconsin, USA). After 48 h puromycin was added, followed by continued incubation for up to 3 weeks, during which puromycin-resistant cells were identified and cloned by limiting dilution.

Protein extraction and sample preparation

Protein extraction, sample preparation, 2D gel electrophoresis and mass spectrometric analysis were performed as published previously (Azizi et al. 2008). To minimise clonal differences, three separate c-myc siRNA clonal transfectants were pooled as well as the three separate siRNA control clones. After pelleting, cells were suspended in 1.0 ml of sample buffer consisting of 7 M urea (Merck, Darmstadt, Germany), 2 M thiourea (Sigma, St. Louis, MO, USA), 4% CHAPS (3-[(3-cholamidopropyl) dimethyl-ammonio]-1-propanesulfonate) (Sigma, St. Louis, MO, USA), 65 mM 1,4-dithioerythritol (Merck, Germany), 1 mM EDTA (ethylenediaminetraacetic acid) (Merck, Germany), protease inhibitors complete® (Roche, Basel, Switzerland) and 1 mM phenylmethylsulfonyl chloride. Sonification of the samples was carried out for approximately 15 s. After homogenisation, samples were left at 20°C for 1 h, and then centrifuged at 14,000×*g* for 1 h. For desalting and protein concentration, the supernatant was transferred into ultrafree-4 centrifugal filter unit (Millipore, Bedford, MA). Protein content of the supernatant was then quantified by Bradford protein assay system (Bradford 1976).

2-D electrophoresis

Six gels of two groups ($n = 3$ per pooled group) were run.

For isoelectric focusing, 800 µg of protein was applied on immobilized pH 3–10 non-linear gradient strips (18 cm, pH range 3–10, Amersham Bioscience, Uppsala, Sweden) at their basic and acidic ends. Focusing was started at 200 V and voltage gradually increased to 8,000 V over 31 h and then kept constant for a further 3 h (approximately 150,000 Vh totally). After the first dimension, strips were equilibrated for 15 min in buffer containing 6 M urea, 20% glycerol, 2% SDS, 2% dithiothreitol (DTT) and then for 15 min in the same buffer containing 2.5% iodo-acetamide instead of DTT.

After equilibration, strips were loaded on 9–16% gradient sodium dodecylsulfate polyacrylamide gels for second-dimensional separation. Gels (180 × 200 × 1.5 mm) were run at 40 mA per gel. Immediately after the second-dimensional electrophoresis, gels were fixed for 18 h in 50% methanol, containing 10% acetic acid, and then stained with colloidal Coomassie blue (Novex, San Diego, CA) for 12 h on a rocking shaker. Molecular masses were determined by running standard protein markers (Bio-Rad Laboratories, Hercules, CA) covering the range 10–250 kDa. Excess of dye was washed out from gels with distilled water and gels were scanned with ImageScanner (Amersham Bioscience).

Quantification

Scans of all gels were imported into software specifically designed for the quantification in proteome analysis (Proteomweaver, Bio-Rad) and spot volume was measured.

Statistical analysis

For each group, the geometric mean of a matched spot was calculated and a Student's *t* test was performed for comparison of the two groups. A spot was seen as significantly up-regulated if the regulation factor was higher than 1.2 (i.e. protein quantity was higher than 120% as compared to controls) and the $p < 0.05$. A spot was significantly down-regulated if the regulation factor was lower than 0.8 (i.e. protein quantity was <80% as compared to controls) and the $p < 0.05$.

In-gel digestion of proteins and protein identification with nano-LC-ESI-Q-TOF mass spectrometry

Gel pieces were cut into small pieces to increase surface and put into a 0.6 ml tube. They were washed with 50 mM ammonium bicarbonate to remove debris, and then washed two times with 50% 50 mM ammonium bicarbonate/50% acetonitrile for 30 min with occasional vortexing. The washing solution was discarded at the end of each wash. 100 µl of 100% acetonitrile was added to each tube covering the gel piece completely and incubated for 5 min. Gel pieces were dried completely in a Speedvac (Eppendorf, Germany). Cysteines were reduced with a 10 mM DTT solution in 0.1 M ammonium bicarbonate for 60 min at 56°C. The same volume of a 55 mM solution of iodoacetamide in 0.1 M ammonium bicarbonate buffer was added and incubated in the dark for 45 min at 25°C to alkylate cysteine residues. The reduction/alkylation solutions were removed by washing with 50 mM ammonium bicarbonate buffer for 10 min. Buffer was removed and the dried gel pieces were re-swollen with 12.5 ng/ml trypsin solution buffered in 25 mM ammonium bicarbonate and incubated for 16 h at 37°C. Supernatants were transferred to new 0.6 ml tubes and gel pieces were extracted subsequently with 50 µl of 0.5% formic acid/20% acetonitrile for 15 min in a sonication bath. The volume was reduced to 10 µl and 20 µl HPLC-water added. Nano-ESI–LC–MS/MS analyses were carried out with the UltiMate 3000 system interfaced to the QSTAR Pulsar mass spectrometer. The gradient was (A = 0.05% trifluoroacetic acid in water, B = 80% acetonitrile/0.04% trifluoroacetic acid in water) from 0 to 50% B in 30 min, 90% B in 5 min, 0% B in 25 min. Peptide spectra were recorded over the mass range of *m/z* 400–1,600, and MS/MS spectra were recorded in information-dependent data acquisition over the mass range of *m/z* 50–1,600. One peptide spectrum was recorded followed by three MS/MS spectra on the QSTAR Pulsar instrument; the accumulation time was 1 s for peptide spectra and 2 s for MS/MS spectra. The collision energy was set automatically according to the mass and charge state of the peptides chosen for fragmentation. Doubly or triply charged peptides were chosen for MS/MS experiments due to their good fragmentation characteristics. MS/MS spectra were interpreted by the MASCOT software (Matrix Science) (Chen et al. 2006).

Verification by Western blot analysis

Western blotting was performed not only for significant proteins, but also for proteins showing a trend after 2D proteome quantification (i.e. a significant but <20% change in protein level: $p < 0.05$, but less than 1.2-fold increase or 0.8 decrease).

Electrophoresis and protein transfer were performed using a Bio-Rad Protean III system (Bio-Rad Laboratories, Hercules, CA). Percentage of the acrylamide gels (acrylamide, Tris 1.5 M, pH 8.8; ddH_20, APS 10%, SDS 10%, TEMED) varied according to the expected protein size of the investigated molecule. Molecular masses were determined by running standard protein markers (Precision Plus, Bio-Rad) covering the range 10–250 kDa. Electrophoresis was performed for 1 h at 40 V, followed by 3–4 h at 60 V in running buffer (Tris 25 mM, glycine 190 mM, SDS 0.1%). Proteins were transferred on to PVDF membranes at 200 mA for 2 h in transfer buffer (Tris 25 mM, glycine 190 mM). Membranes were blocked with 5% dry milk in TBST (Tris 20 mM, NaCl 0.137 M, TWEEN-20 0.1%, HCl 0.04%) for 1 h.

Primary antibodies (listed in Table 1) were applied as recommended by the manufacturer and incubated overnight at 4°C. After washing, the HRP-conjugated secondary antibody was added in 5% milk-TBST for 1 h. Chemiluminescence of the Western blots was directly acquired from the ChemiDoc XRS camera (Bio-Rad) into the specific 1D quantification software, Quantity One (Bio-Rad).

Beta-actin was used as loading control.

Results

siRNA

D425Med cells were successfully transfected with c-myc siRNA constructs, leading to down-regulation of endogenous c-myc expression as shown by Western blotting (Fig. 1). Six clonal transfectants were generated using limiting dilution: Three of these clonal transfectants were c-myc

Table 1 Primary antibodies used for Western blotting

Antigen	Species	Protein size (kDa)	Dilution	Manufacturer
Actin, beta	Mouse	42	1:4,000	Sigma
ALDH2	Mouse	56	1:10,000	Sigma
ARD1A	Mouse	26	1:500	Abnova
Calponin-3	Rabbit	34	1:2,000	Santa-Cruz
Cofilin	Mouse	19	1:500	TD
ERp29	Rabbit	29	1:2,000	Acris
ERp29	Rabbit	29	1:5,000	ABR
GAMT	Rabbit	26	1:250	Santa-Cruz
hnRNP A/B	Rabbit	35	1:2,000	Aviva
hnRNP C1/C2	Mouse	43	1:5,000	Sigma
Myc (c-myc)	Mouse	62	1:2,000	Pharmingen
PEBP1	Rabbit	18	1:1,000	Sigma
PQBP1	Rabbit	38	1:1,000	Sigma
PRDX4	Rabbit	25	1:2,000	Abnova
RPLP1	Rabbit	15	1:500	Sigma
Stathmin	Mouse	19	1:250	TD
STIP-1	Mouse	63	1:5,000	Sigma
TARDBP	Mouse	55	1:5,000	Abnova
THOC3	Rabbit	45	1:250	Santa-Cruz
TPI1	Mouse	27	1:2,000	Sigma
UCHL1	Mouse	25	1:10,000	Sigma

siRNA clones (clones D9, E7, H10), whereas the other three clonal transfectants consisted of Silencer® negative control siRNA clones (Ambion), carrying a siRNA that did not target any gene product (clones C6, C9, D4).

Differential proteomics and Western blot analysis

Images of a representative 2DE images of sample gel from the control group and the myc-downregulated group are shown in Fig. 2. Analysis with Proteomweaver software revealed 36 differentially expressed protein spots. Q-TOF analysis was performed on these spots in one sample gel of each group.

Eight out of these were shown to be complex protein mixtures, and these were not further analysed by Western blotting along with six spots that could not be identified due to technical reasons in terms of low sequence coverage or low scores. The remaining 22 spots represented 22 individual proteins. Tables 2 and 3 show the difference between protein levels in both groups. Data revealing protein identification are shown in Tables 4 and 5 and peptides matching are listed in supplemental table 1.

Q-TOF analysis led to the identification of 23 different proteins. 11 proteins corresponded to increased spots: 39S ribosomal protein L12 mitochondrial precursor (UniProt ID: P52815; increased 1.52-fold, $p = 0.005$), acyl-protein thioesterase 1 (UniProt ID: O75608; increased 1.29-fold, $p = 0.0334$), cofilin-1 (UniProt ID: P23528; increased 1.47-fold, $p = 0.0358$), heterogeneous nuclear ribonucleoprotein A/B (UniProt ID: Q99729; increased 1.18-fold, $p = 0.0402$), heterogeneous nuclear ribonucleoproteins C1/C2 (UniProt ID: P07910; increased 1.26-fold, $p = 0.005$), phosphatidylethanolamine-binding protein 1 (PEBP1; UniProt ID: P30086; increased 1.29-fold, $p = 0.0334$), n-MYC downstream-regulated gene 1 (NDRG1; UniProt ID: P60709; increased 1.29-fold, $p = 0.0304$), stathmin (UniProt ID: P16949; increased 1.23-fold, $p = 0.0321$), stress-induced-phosphoprotein 1 (STIP1; UniProt ID: P31948; increased 1.37-fold, $p = 0.0111$), triosephosphate isomerase (TPI1; UniProt ID: P60174; increased 1.57-fold, $p = 0.0088$) and ubiquitin carboxyl-terminal hydrolase isozyme L1 (UCHL1; UniProt ID: P09936; increased 1.37-fold, $p = 0.0158$). Eleven proteins corresponded to decreased spots: 60S acidic ribosomal protein P0 (UniProt ID: P05388; decreased 0.55-fold, $p = 0.0426$ and 0.27-fold, $p = 0.036$), aldehyde dehydrogenase mitochondrial precursor (ALDH2; UniProt ID: P05091; decreased 0.75-fold, $p = 0.003$), calponin-3 (UniProt ID: Q15417; decreased 0.62-fold, $p = 0.0049$), endoplasmic reticulum protein ERp29 precursor (UniProt ID: P30040; decreased 0.78-fold, $p = 0.0413$), guanidinoacetate *N*-methyltransferase (GAMT; UniProt ID: Q14353; decreased 0.85-fold,

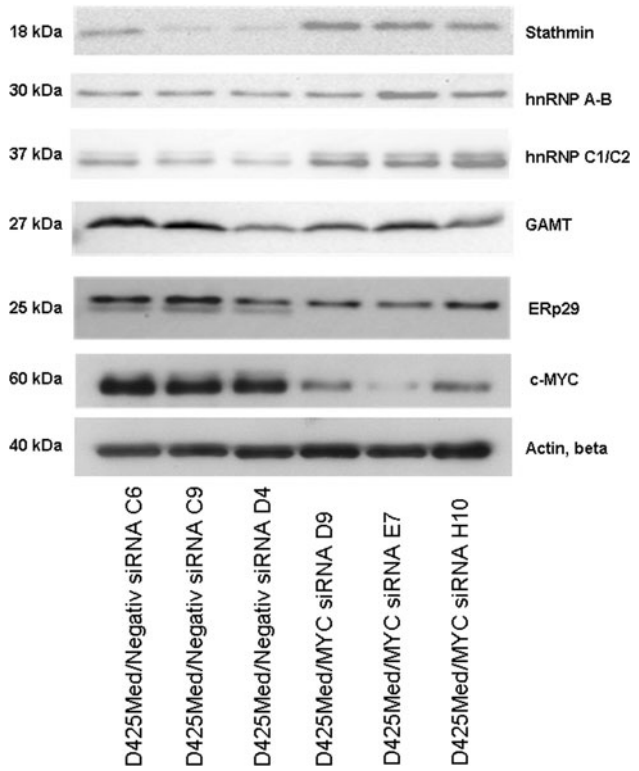

Fig. 1 Western blot analysis of c-myc, stathmin, heterogeneous nuclear ribonucleoprotein A/B (hnRNP A/B), heterogeneous nuclear ribonucleoproteins C1/C2 (hnRNP C1/C2), guanidinoacetate *N*-methyltransferase (GAMT), endoplasmic reticulum protein ERp29 and beta-actin (loading control) expression in D425Med clonal transfectants

$p = 0.0457$), N-terminal acetyltransferase complex ARD1 subunit homologue A (ARD1A; UniProt ID: P41227; decreased 0.61-fold, $p = 0.0234$), peroxiredoxin-4 (PRD X4;UniProt ID: Q13162; decreased 0.70-fold, $p = 0.0271$), polyglutamine-binding protein 1 (PQBP1; UniProt ID: O60828; decreased 0.76-fold, $p = 0.0076$), TAR DNA-binding protein 43 (TARDBP; UniProt ID: Q13148; decreased 0.78-fold, $p = 0.0362$) and THO complex subunit 3 (UniProt ID: Q96J01; decreased 0.59-fold, $p = 0.0076$).

Western blotting was performed for confirmation and bands quantified in silico (Fig. 1; Table 6). Three proteins showed higher arbitrary units of optical density of bands in the c-myc silenced clones. Heterogeneous nuclear ribonucleoproteins C1/C2 (UniProt ID: P07910; 1.66-fold), stathmin (UniProt ID: P16949; 2.04-fold) and heterogeneous nuclear ribonucleoprotein A/B (UniProt ID: Q99729; 1.55-fold) matched the findings of Proteomweaver analysis. Levels of six proteins were comparable, whilst no suitable antibodies were available for three proteins.

Two proteins (endoplasmic reticulum protein ERp29 precursor (UniProt ID: P30040; 0.69-fold) and guanidino acetate *N*-methyltransferase (UniProt ID: Q14353; 0.80-fold) were found decreased by Western blotting concordantly to *Proteomweaver* analysis. Levels of eight proteins were comparable, whilst no suitable antibody was available for one protein.

The results are summarised in Tables 2, 3, 4, 5, 6.

Discussion

As demonstrated in the "Results" section five proteins from several pathways were differentially expressed between control and c-myc D425Med MB cells as shown by a gel-based proteomics method and verification by Western blotting.

Different protein levels may indicate involvement of different c-myc-dependent pathways or at least reveal c-myc-dependent modification of the five protein levels. These proteins may directly depend on c-myc intracellular

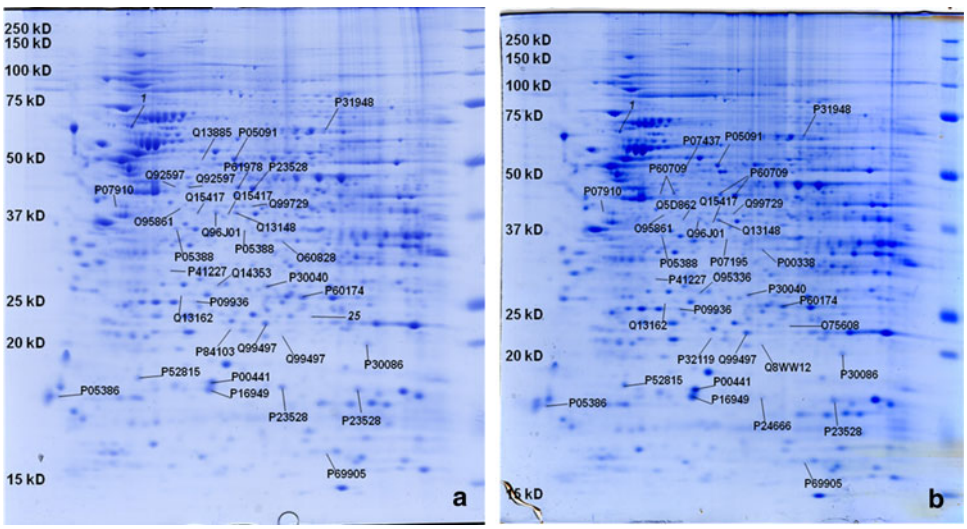

Fig. 2 Two representative master gels of two groups are shown. **a** 2D SDS–PAGE of D425Med control cells. Differentially expressed spots as well as accession numbers from UniProtKB of proteins identified by Q-TOF analysis are indicated. **b** 2D SDS–PAGE of D425Med cells after c-myc down-regulation. Differentially expressed spots as well as accession numbers of proteins identified by Q-TOF analysis are indicated. *X* axis indicates apparent molecular weight, *Y* axis the pH range from 3 to 10

Table 2 Proteins showing increased levels in the c-myc silenced group

Control		c-myc down-regulation		Fold change	*t* test	Control					c-myc up-regulation					Western blot
Accession no.	Protein name	Accession no.	Protein name			1	2	3	Mean	SD	1	2	3	Mean	SD	
P60174	Triosephosphate isomerase	P60174	Triosephosphate isomerase	1.57	0.0088	0.154	0.164	0.13	0.1493	0.0175	0.250	0.215	0.238	0.2343	0.0178	⇔
P52815	Keratin, type II cytoskeletal; 3rd best hit 39S ribosomal protein L12, mitochondrial precursor	P52815	39S ribosomal protein L12, mitochondrial precursor	1.52	0.0050	0.622	0.526	0.572	0.5733	0.0480	0.828	0.971	0.817	0.8720	0.0859	n.d.
P23528	Cofilin-1	P23528	Cofilin-1	1.47	0.0358	1.069	0.866	1.164	1.0330	0.1522	1.404	1.789	1.359	1.5173	0.2363	⇔
P09936	Ubiquitin carboxyl-terminal hydrolase isozyme L1	P09936	Ubiquitin carboxyl-terminal hydrolase isozyme L1	1.37	0.0158	0.357	0.385	0.317	0.3530	0.0342	0.434	0.496	0.521	0.4837	0.0448	⇔
P31948	Stress-induced-phosphoprotein 1	P31948	Stress-induced-phosphoprotein 1	1.37	0.0111	0.345	0.292	0.335	0.3240	0.0282	0.437	0.481	0.412	0.4433	0.0349	⇔
P30086	Phosphatidylethanolamine-binding protein 1	P30086	Phosphatidylethanolamine-binding protein 1	1.29	0.0334	0.524	0.593	0.651	0.5893	0.0636	0.699	0.767	0.820	0.7620	0.0607	⇔
Q92597	Protein NDRG1	P60709	Actin, cytoplasmic 1, 2nd best hit: Protein NDRG1	1.29	0.0304	0.227	0.187	0.194	0.2027	0.0214	0.287	0.255	0.244	0.2620	0.0223	⇔
	No match	O75608	Acyl-protein thioesterase 1	1.29	0.0334	0.524	0.593	0.651	0.5893	0.0636	0.767	0.693	0.820	0.7600	0.0638	n.d.
P07910	**Heterogeneous nuclear ribonucleoproteins C1/C2**	**P07910**	**Heterogeneous nuclear ribonucleoproteins C1/C2**	**1.26**	**0.0050**	**4.647**	**3.908**	**3.761**	**4.1053**	**0.4748**	**5.212**	**5.216**	**5.095**	**5.1743**	**0.0687**	⇧
P16949	**Stathmin**	**P16949**	**Stathmin**	**1.23**	**0.0321**	**2.016**	**2.073**	**2.097**	**2.0620**	**0.0416**	**2.482**	**2.858**	**2.289**	**2.5430**	**0.2894**	⇧
Q99729	**Heterogeneous nuclear ribonucleoprotein A/B**	**Q99729**	**Heterogeneous nuclear ribonucleoprotein A/B**	**1.18**	**0.0402**	**0.214**	**0.227**	**0.216**	**0.2190**	**0.0070**	**0.276**	**0.240**	**0.259**	**0.2583**	**0.0180**	⇧

Numbers 1–3 indicate individual gels per group

Changes confirmed by Western blotting are marked bold

Table 3 Proteins showing decreased levels in the c-myc silenced group

Control		c-myc down-regulation		Fold change	*t* test	Control					c-myc down-regulation					Western blot
Accession no.	Protein name	Accession no.	Protein name			1	2	3	Mean	SD	1	2	3	Mean	SD	
Q14353	**Guanidinoacetate *N*-methyltransferase**	**O95336**	6-Phosphogluconolactonase, **3rd best hit: Guanidinoacetate *N*-methyltransferase**	**0.85**	**0.0457**	**0.551**	**0.636**	**0.584**	**0.5903**	**0.0429**	**0.522**	**0.491**	**0.491**	**0.5013**	**0.0179**	⇩
Q13148	TAR DNA-binding protein 43	Q13148	TAR DNA-binding protein 43	0.78	0.0362	0.463	0.400	0.483	0.4487	0.0433	0.366	0.310	0.369	0.3483	0.0332	⇔
P30040	**Endoplasmic reticulum protein ERp29 precursor**	**P30040**	**Endoplasmic reticulum protein ERp29 precursor**	**0.78**	**0.0413**	**0.669**	**0.669**	**0.619**	**0.6523**	**0.0289**	**0.456**	**0.567**	**0.496**	**0.5063**	**0.0562**	⇩
O60828	Polyglutamine-binding protein 1	P00338	L-Lactate dehydrogenase A chain, 2nd best hit: polyglutamine-binding protein 1	0.76	0.0076	0.449	0.389	0.415	0.4177	0.0301	0.299	0.317	0.334	0.3167	0.0175	⇔
P05091	Aldehyde dehydrogenase, mitochondrial precursor 4	P05091	Aldehyde dehydrogenase, mitochondrial precursor 4	0.75	0.0030	0.987	1.039	1.065	1.0303	0.0397	0.738	0.823	0.763	0.7747	0.0437	⇔
Q13162	Peroxiredoxin-4	Q13162	Peroxiredoxin-4	0.70	0.0271	0.149	0.175	0.133	0.1523	0.0212	0.096	0.116	0.108	0.1067	0.0101	⇔
Q15417	Calponin-3	Q15417	Calponin-3	0.62	0.0049	0.104	0.179	0.155	0.1460	0.0383	0.102	0.094	0.077	0.0910	0.0128	⇔
P41227	N-terminal acetyltransferase complex ARD1 subunit homologue A	P41227	N-terminal acetyltransferase complex ARD1 subunit homologue A	0.61	0.0234	0.184	0.253	0.221	0.2193	0.0345	0.156	0.137	0.109	0.1340	0.0236	⇔
Q96J01	THO complex subunit 3	Q96J01	THO complex subunit 3	0.59	0.0076	0.352	0.384	0.455	0.3970	0.0527	0.223	0.269	0.211	0.2343	0.0306	⇔
P05386	60S acidic ribosomal protein P1	P05386	60S acidic ribosomal protein P1	0.55	0.0426	0.799	0.646	0.545	0.6633	0.1279	0.877	0.104	0.108	0.3629	0.4452	⇔
P05388	60S acidic ribosomal protein P0	P05388	60S acidic ribosomal protein P0	0.27	0.0360	0.280	0.986	0.239	0.5017	0.4199	0.195	0.100	0.113	0.1360	0.0515	n.d.

Numbers 1–3 indicate individual gels per group

Changes confirmed by Western blotting are marked bold

Table 4 List of proteins identified by Q-TOF in the control group

Spot	Protein ID	Protein name	Mass	Score
1	Not identified			
2	**STIP1_HUMAN**	**Stress-induced-phosphoprotein 1**	**63,227**	**657**
3	K2C8_HUMAN	Keratin, type II cytoskeletal 8	53,671	437
4	**ALDH2_HUMAN**	**Aldehyde dehydrogenase, mitochondrial precursor**	**56,859**	**1,176**
5	**NDRG1_HUMAN**	**Protein NDRG1**	**43,264**	**140**
6	NDRG1_HUMAN	Protein NDRG1	43,264	271
7	HNRPK_HUMAN	Heterogeneous nuclear ribonucleoprotein K	51,230	215
8	COF1_HUMAN	Cofilin-1, Homo sapiens	18,719	60
9	K2C1_HUMAN	Heterogeneous nuclear ribonucleoproteins C1/C2	33,707	302
10	CNN3_HUMAN	Calponin-3	36,562	76
11	**CNN3_HUMAN**	**Calponin-3**	**36,562**	**258**
12	**ROAA_HUMAN**	**Heterogeneous nuclear ribonucleoprotein A/B**	**36,316**	**220**
13	BPNT1_HUMAN	3'(2'),5'-bisphosphate nucleotidase 1	33,713	78
14	**THOC3_HUMAN**	**THO complex subunit 3**	**39,431**	**101**
15	**TADBP_HUMAN**	**TAR DNA-binding protein 43**	**45,053**	**56**
16	**RLA0_HUMAN**	**60S acidic ribosomal protein P0**	**34,423**	**349**
17	RLA0_HUMAN	60S acidic ribosomal protein P0	34,423	177
18	**PQBP1_HUMAN**	**Polyglutamine-binding protein 1**	**30,511**	**106**
19	**ARD1A_HUMAN**	**N-terminal acetyltransferase complex ARD1 subunit homologue A**	**26,613**	**60**
20	**GAMT_HUMAN**	**Guanidinoacetate *N*-methyltransferase**	**26,529**	**187**
21	**ERP29_HUMAN**	**Endoplasmic reticulum protein ERp29 precursor**	**29,032**	**296**
22	**PRDX4_HUMAN**	**Peroxiredoxin-4**	**30,749**	**220**
23	**UCHL1_HUMAN**	**Ubiquitin carboxyl-terminal hydrolase isozyme L1**	**25,151**	**243**
24	**TPIS_HUMAN**	**Triosephosphate isomerase**	**26,938**	**586**
25	Not identified			
26	SFRS3_HUMAN	Splicing factor, arginine/serine-rich 3	19,546	72
27	**PARK7_HUMAN**	**Protein DJ-1**	**20,050**	**58**
28	PARK7_HUMAN	Protein DJ-1	20,050	58
29	**PEBP1_HUMAN**	**Phosphatidylethanolamine-binding protein 1**	**21,158**	**428**
30	K2C1_HUMAN	Keratin, type II cytoskeletal 1	66,149	158
31	**RM12_HUMAN**	**39S ribosomal protein L12, mitochondrial precursor**	**21,563**	**137**
32	**STMN1_HUMAN**	**Stathmin**	**17,292**	**214**
33	**SODC_HUMAN**	**Superoxide dismutase [Cu–Zn]**	**16,154**	**238**
34	COF1_HUMAN	Cofilin-1	18,719	385
35	**COF1_HUMAN**	**Cofilin-1**	**18,719**	**276**
36	K22E_HUMAN	Keratin, type II cytoskeletal 2 epidermal	66,110	328

Protein spots concordantly identified in the c-myc-downregulated as well as the control group are marked bold

levels per se or indirectly represent changes mediated by decreased c-myc levels.

Data obtained in this study may now be tested in primary tumours to evaluate the potential of dysregulated proteins, as tentative marker candidates for tumour classification or dignity.

It is not surprising that only 5 out of 32 protein levels from the gel-based proteomics technique could be verified by Western blotting, because both methods show inherent flaws. Protein spots may contain more than one protein and Western blotting depends on specificity of antibodies. Most antibodies are not specific or do not react with protein isoforms or proteins showing posttranslational modifications. Ideally, antibody specificity should be unambiguously characterised as proposed recently (Heo and Lubec 2010). Moreover, many expression forms of proteins (splice variants or modified proteins) would be separated on 2 DE, but the simple use of SDS–PAGE would not separate them and

Table 5 List of proteins identified by Q-TOF in the c-myc down-regulated group

Spot	Protein ID	Protein name	Mass	Score
1	Not identified			
2	**STIP1_HUMAN**	**Stress-induced-phosphoprotein 1**	**63,227**	**520**
3	TBB5_HUMAN	Tubulin beta chain	50,095	80
4	**ALDH2_HUMAN**	**Aldehyde dehydrogenase, mitochondrial precursor**	**56,859**	**1,059**
5	**NDRG1_HUMAN**	**Protein NDRG1**	**43,264**	**90**
6	ACTB_HUMAN	Actin, cytoplasmic 1	42,052	160
7	ACTB_HUMAN	Actin, cytoplasmic 1	42,052	156
8	ACTB_HUMAN	Actin, cytoplasmic 1	42,052	101
9	HNRPC_HUMAN	Heterogeneous nuclear ribonucleoproteins C1/C2	33,707	365
10	K22E_HUMAN	Keratin, type II cytoskeletal 2 epidermal	66,110	1,210
11	**CNN3_HUMAN**	**Calponin-3**	**36,562**	**268**
12	**ROAA_HUMAN**	**Heterogeneous nuclear ribonucleoprotein A/B**	**36,316**	**200**
13	K2C1_HUMAN	Keratin, type II cytoskeletal 1	66,149	465
14	**THOC3_HUMAN**	**THO complex subunit 3**	**39,431**	**273**
15	**TADBP_HUMAN**	**TAR DNA-binding protein 43**	**45,053**	**198**
16	**RLA0_HUMAN**	**60S acidic ribosomal protein P0—Homo sapiens**	**34,423**	**390**
17	LDHB_HUMAN	L-Lactate dehydrogenase B chain	36,900	330
18	**PQBP1_HUMAN**	**Polyglutamine-binding protein 1**	**30,511**	**210**
19	**ARD1A_HUMAN**	**N-terminal acetyltransferase complex ARD1 subunit homologue A**	**26,613**	**349**
20	**GAMT_HUMAN**	**Guanidinoacetate *N*-methyltransferase**	**26,529**	**357**
21	**ERP29_HUMAN**	**Endoplasmic reticulum protein ERp29 precursor**	**29,032**	**503**
22	**PRDX4_HUMAN**	**Peroxiredoxin-4**	**30,749**	**262**
23	**UCHL1_HUMAN**	**Ubiquitin carboxyl-terminal hydrolase isozyme L1**	**25,151**	**381**
24	**TPIS_HUMAN**	**Triosephosphate isomerase**	**26,938**	**706**
25	**LYPA1_HUMAN**	**Acyl-protein thioesterase 1**	**24,996**	**231**
26	K2C1_HUMAN	Keratin, type II cytoskeletal 1	66,149	403
27	**PARK7_HUMAN**	**Protein DJ-1**	**20,050**	**715**
28	PCNP_HUMAN	PEST proteolytic signal-containing nuclear protein	18,913	219
29	**PEBP1_HUMAN**	**Phosphatidylethanolamine-binding protein 1**	**21,158**	**443**
30	RLA1_HUMAN	60S acidic ribosomal protein P1	11,621	86
31	**RM12_HUMAN**	**39S ribosomal protein L12, mitochondrial precursor**	**21,563**	**151**
32	**STMN1_HUMAN**	**Stathmin**	**17,292**	**176**
33	**SODC_HUMAN**	**Superoxide dismutase [Cu–Zn]**	**16,154**	**268**
34	PPAC_HUMAN	Low molecular weight phosphotyrosine protein phosphatase	18,487	231
35	**COF1_HUMAN**	**Cofilin-1**	**18,719**	**403**
36	K1C10_HUMAN	Keratin, type I cytoskeletal 10	59,703	417

Protein spots concordantly identified in the c-myc-downregulated as well as the control group are marked bold

therefore, quantification of such a single immunoreactive band would not show results comparable to quantification from 2DE gels.

Levels of the *heterogeneous nuclear ribonucleoproteins* (*hnRNP*) *C1/C2* and *A/B* were increased after c-myc down-regulation. Both proteins are part of the telomerase complex and overexpression of hnRNP C1/C2 leads to shortening of telomere length (MacLeod et al. 2004; Meffert et al. 2005). The increased protein levels in experiments herein may support the findings of von Bueren et al. (2009) that c-myc knock-down is leading to decreased telomerase activity in MB cell lines. hnRNPs are also involved in DNA damage repair (reviewed by Haley et al. 2009) and up-regulation of hnRNP C1/C2 has previously been shown in cancer, e.g. in hepatocellular carcinoma (Sun et al. 2007) and in neuronal cells surviving apoptotic (ischaemic) stress (Spahn et al. 2008). Down-regulation of the hnRNP C1/C2 protein amount was reported in acute promyelocytic leukaemia upon treatment with all-*trans*-retinoic acid (Harris et al. 2004). Decrease in hnRNP C1/

Table 6 Volume of Western blot protein bands as measured by quantity one 1D software

	Control clone 1	Control clone 2	Control clone 3	Median control	myc down-regulated clone 1	myc down-regulated clone 2	myc down-regulated clone 3	Median myc down-regulated	Ratio down-regulated: control
Stathmin	7,563.32	5,278.40	3,502.44	5,448.05	13,471.36	10,378.04	9,411.88	11,087.09	2.04
hnRNP A/B	10,660.04	10,744.56	10,535.96	10,646.85	12,371.60	22,726.92	14,402.00	16,500.18	1.55
hnRNP C1/C2	122,770.21	94,698.57	84,588.57	100,685.78	172,747.18	145,839.26	182,105.14	166,897.19	1.66
GAMT	176,670.64	174,112.93	84,548.17	145,110.58	116,443.09	147,574.81	82,180.54	115,399.48	0.80
ERp29	41,205.36	39,354.36	22,796.92	34,452.22	24,158.12	17,987.60	29,509.04	23,884.92	0.69

C2 levels itself was correlated to higher sensitivity towards chemical stress (Hossain et al. 2007). HnRNP C1/C2 was proven to bind to p53 mRNA and this binding is strongly enhanced in response to cytotoxic drugs, which increase cytosolic hnRNP C1/C2 levels (Christian et al. 2008). Correlation of these levels to mRNA binding, although, could not be demonstrated (Christian et al. 2008). An increase in hnRNP levels may also lead to a decrease in radiation sensitivity (Haley et al. 2009). Together, these findings may explain the reduction in radiation and chemosensitivity in MB cell lines by c-myc downregulation as demonstrated by van Bueren et al. (2009).

HnRNP C1/C2 was proven to be important for correct progression through the cell cycle and its decrease led to cell cycle arrest at G2/M. Translation of c-myc has been shown to be influenced in a cell cycle-dependent manner by binding of hnRNP C1/C2 to an internal ribosomal entry site (IRES) of c-myc mRNA (Kim et al. 2003). The addition of hnRNP C1 led to an increase in c-myc protein expression in vitro (Kim et al. 2003). It, therefore, remains unclear, whether changes in hnRNP C1/C2 levels demonstrated in the current experiments represent a true direct down-stream effect of c-myc or could be seen as a feedback loop reflecting an attempt of the cell to compensate for the dropping c-myc protein levels after c-myc silencing.

Stathmin (also known as oncoprotein 18 or OP18) is a tubulin depolymerising protein reviewed by Rubin and Atweh (2004). Stathmin prevents the correct formation of the mitotic spindle that can only form after phosphorylation of the protein. On the other hand, dephosphorylation at the end of mitosis induces correct spindle depolymerisation. Stathmin is under control of p53 and p53 induction leads to stathmin down-regulation, thus possibly contributing to p53-induced growth inhibition (Ahn et al. 1999). In addition to its mitotic function, stathmin has been associated with neuronal cell motility (Giampietro et al. 2005; Jin et al. 2004).

Differential expression of stathmin has repeatedly been described in various cancer types, such as leukaemia (Melhem et al. 1991), lung adenocarcinoma (Chen et al. 2003), oral squamous-cell carcinoma (Kouzu et al. 2006), hepatocellular carcinoma (Yuan et al. 2006), ovarian cancer (Wei et al. 2008), breast cancer (Alli et al. 2007b; Brattsand 2000), Wilms tumours (Takahashi et al. 2002), and glioblastoma multiforme (Ngo et al. 2007). Stathmin overexpression was associated with poor outcome and a more malignant phenotype. Cell proliferation and oestrogen receptor negativity was associated with stathmin positivity in breast cancer (Brattsand 2000) and stathmin silencing decreased breast cancer cell proliferation and viability (Alli et al. 2007b). In Wilms tumours, stathmin was expressed in higher levels increasing with tumour grade (Takahashi et al. 2002). Proteomics and mRNA expression analysis revealed stathmin overexpression in lung adenocarcinoma as compared to normal tissue, with an increase in phosphorylation. Stathmin overexpression correlated with poor differentiation in this malignancy (Chen et al. 2003). Similar results were found in oral squamous-cell carcinoma: stathmin protein and mRNA, and immunohistochemical expression of stathmin was higher than in normal tissue and a correlation between high protein expression and poor prognosis was described (Kouzu et al. 2006). In hepatocellular carcinoma, elevated stathmin levels were accompanied by a more aggressive behaviour (Yuan et al. 2006). Metastatic cases of ovarian cancer harboured higher levels of stathmin (Wei et al. 2008). In a mouse glioblastoma multiforme model, stathmin was correlated with poor survival and resistance to nitrosourea compounds (Ngo et al. 2007).

In MB, stathmin down-regulation was seen in DAOY cells upon apoptosis induced by methionine deprivation (Kokkinakis et al. 2004). Previously published own work identified stathmin down-regulation after stimulation of TrKC-transfected DAOY cells by addition of its substrate, neurotrophin 3 (Gruber-Olipitz et al. 2009). Neurotrophin receptor TrkC is a known prognostic marker in MB, where its high expression correlates with better survival (Grotzer et al. 2001; Rutkowski et al. 2007). Kuo et al. (2009) and

Neben et al. (2004) independently described high stathmin expression in MB to correlate with a fulminant course of disease and frequent dissemination.

Recent publications focus on stathmin's role in anti-cancer therapy. It diminishes the action of microtubule destabilising agents, such as vinca alkaloids and taxanes (Hait and Yang 2006) and its down-regulation reverses susceptibility to these drugs as shown in breast cancer cells (Alli et al. 2007a). Its inhibition was reported to contribute synergistically to taxol-induced antiproliferative and migratory effects of endothelial cells, suggesting a possible therapeutic anti-angiogenic potential of anti-stathmin agents (Mistry et al. 2007).

No connection or correlation between c-myc and stathmin has been reported so far and herein increased levels of stathmin in D425Med cells upon c-myc knock-down are revealed.

Guanidinoacetate N-methyltransferase (*GAMT*), down-regulated in our experiments, is a key enzyme of creatine metabolism as reviewed by Braissant et al. (2007) and its deficiency is associated with inborn neurologic disorders (cerebral creatine deficiency syndromes, CCDSs) (Stockler et al. 2007). Creatine is involved in cellular energy metabolism and ATP homeostasis and is essential for neuronal cells. Changes in creatine metabolism have been described in various malignancies, such as hepatocellular or cervical carcinoma, where an elevation of brain-type creatine-kinase was described (Choi et al. 2001; Meffert et al. 2005). Recently, Ide et al. (2009) established that GAMT activity is p53-dependent and contributes to apoptosis in conditions of glucose starvation or nutrient stress. Reduction in GAMT observed in our experiments may have contributed to the reduction in apoptosis seen in MB cell lines by van Bueren et al. (2009) after c-myc silencing.

Endoplasmic reticulum protein ERp29 levels were decreased in our experiments. It is localised in the endoplasmic reticulum and was primarily described as a chaperone for secretory proteins, including thyroglobulin (Sargsyan et al. 2002) and is ubiquitously expressed with brain levels higher as compared to other organs (MacLeod et al. 2004).

Mkrtchian et al. (2008) showed that ERp29 downregulation led to volume reduction in breast cancer xenografts. These results were gained by two alternative methods: transfection of breast cancer cells with a dominant-negative ERp29 variant or ERp29 overexpression as well as gene silencing using siRNA techniques. Xenograft cells with the dominant-negative ERp29 isoform furthermore exhibited a higher differentiation and were smaller, but cell growth in vitro was unchanged as compared to wild type or over-expressing cells (Mkrtchian et al. 2008). These findings are in disagreement with those by Bambang et al. describing ERp29 as putative tumour suppressor in breast cancer due to its ability to reduce xenograft growth in nude mice, arrest cells at G0/G1 and inhibit cell proliferation (Bambang et al. 2009). ERp29 has also been identified in other malignancies, such as in hepatocarcinoma cells (Feng et al. 2007) or basal-cell carcinoma (Cheretis et al. 2006). In this pathology, the degree of infiltration and malignancy was correlated to a higher ERp29 expression. The role of ERp29 in MB cells remains as yet to be elucidated. Its decrease upon c-myc knock-down may suggest its implication in the development of more aggressive behaviour.

Conclusions

c-myc knock-down in D425Med cells using siRNA leads to measurable differences in the level of a variety of proteins from several pathways and families as identified by 2D gel electrophoresis and mass spectrometric analysis. For five proteins, these findings could be confirmed by Western blot analysis. Levels of hnRNP A/B, hnRNP C1/C2 and stathmin were increased after c-myc down-regulation; those of GAMT, ERp29 were decreased. The biological role of these proteins in MB cells will have to be studied in further downstream experiments. The investigation will have to be extended to primary tumour material and protein expression should ultimately be correlated to patient outcome to allow better risk stratification and therapy planning in children with MB.

Acknowledgments This work was mainly financed by a grant of the *Jubiläumsfonds der Österreichische Nationalbank* (*OeNB*) (Jubiläumsfondsprojekt Nr. 12195). The project was in part supported by the *Forschungsgesellschaft für cerebrale Tumore.*

Conflict of interest The authors state that there is no conflict of interests.

References

Ahn J, Murphy M, Kratowicz S, Wang A, Levine AJ, George DL (1999) Down-regulation of the stathmin/Op18 and FKBP25 genes following p53 induction. Oncogene 18:5954–5958

Aldosari N, Bigner SH, Burger PC, Becker L, Kepner JL, Friedman HS, McLendon RE (2002) MYCC and MYCN oncogene amplification in medulloblastoma. A fluorescence in situ hybridization study on paraffin sections from the Children's Oncology Group. Arch Pathol Lab Med 126:540–544

Alli E, Yang JM, Ford JM, Hait WN (2007a) Reversal of stathmin-mediated resistance to paclitaxel and vinblastine in human breast carcinoma cells. Mol Pharmacol 71:1233–1240

Alli E, Yang JM, Hait WN (2007b) Silencing of stathmin induces tumor-suppressor function in breast cancer cell lines harboring mutant p53. Oncogene 26:1003–1012

Azizi AA, Kang SU, Freilinger A, Gruber-Olipitz M, Chen WQ, Yang JW, Hengstschlager M, Slavc I, Lubec G (2008) Mitosis-

dependent protein expression in neuroblastoma cell line N1E–115. J Proteome Res 7:3412–3422

Bambang IF, Xu S, Zhou J, Salto-Tellez M, Sethi SK, Zhang D (2009) Overexpression of endoplasmic reticulum protein 29 regulates mesenchymal–epithelial transition and suppresses xenograft tumor growth of invasive breast cancer cells. Lab Invest 89:1229–1242

Bradford MM (1976) A rapid and sensitive method for the quantitation of microgram quantities of protein utilizing the principle of protein-dye binding. Anal Biochem 72:248–254

Braissant O, Bachmann C, Henry H (2007) Expression and function of AGAT, GAMT and CT1 in the mammalian brain. Subcell Biochem 46:67–81

Brattsand G (2000) Correlation of oncoprotein 18/stathmin expression in human breast cancer with established prognostic factors. Br J Cancer 83:311–318

Bullions LC, Levine AJ (1998) The role of beta-catenin in cell adhesion, signal transduction, and cancer. Curr Opin Oncol 10:81–87

Chapman CA, Waber DP, Bernstein JH, Pomeroy SL, LaVally B, Sallan SE, Tarbell N (1995) Neurobehavioral and neurologic outcome in long-term survivors of posterior fossa brain tumors: role of age and perioperative factors. J Child Neurol 10:209–212

Chen G, Wang H, Gharib TG, Huang CC, Thomas DG, Shedden KA, Kuick R, Taylor JM, Kardia SL, Misek DE, Giordano TJ, Iannettoni MD, Orringer MB, Hanash SM, Beer DG (2003) Overexpression of oncoprotein 18 correlates with poor differentiation in lung adenocarcinomas. Mol Cell Proteomics 2:107–116

Chen WQ, Kang SU, Lubec G (2006) Protein profiling by the combination of two independent mass spectrometry techniques. Nat Protoc 1:1446–1452

Cheretis C, Dietrich F, Chatzistamou I, Politi K, Angelidou E, Kiaris H, Mkrtchian S, Koutselini H (2006) Expression of ERp29, an endoplasmic reticulum secretion factor in basal-cell carcinoma. Am J Dermatopathol 28:410–412

Choi H, Park CS, Kim BG, Cho JW, Park JB, Bae YS, Bae DS (2001) Creatine kinase B is a target molecule of reactive oxygen species in cervical cancer. Mol Cells 12:412–417

Christian KJ, Lang MA, Raffalli-Mathieu F (2008) Interaction of heterogeneous nuclear ribonucleoprotein C1/C2 with a novel cis-regulatory element within p53 mRNA as a response to cytostatic drug treatment. Mol Pharmacol 73:1558–1567

Claassen GF, Hann SR (1999) Myc-mediated transformation: the repression connection. Oncogene 18:2925–2933

Das P, Puri T, Suri V, Sharma MC, Sharma BS, Sarkar C (2009) Medulloblastomas: a correlative study of MIB-1 proliferation index along with expression of c-Myc, ERBB2, and anti-apoptotic proteins along with histological typing and clinical outcome. Childs Nerv Syst 25:825–835

Dennis M, Spiegler BJ, Hetherington CR, Greenberg ML (1996) Neuropsychological sequelae of the treatment of children with medulloblastoma. J Neurooncol 29:91–101

Eberhart CG, Tihan T, Burger PC (2000) Nuclear localization and mutation of beta-catenin in medulloblastomas. J Neuropathol Exp Neurol 59:333–337

Ellison DW, Onilude OE, Lindsey JC, Lusher ME, Weston CL, Taylor RE, Pearson AD, Clifford SC (2005) Beta-catenin status predicts a favorable outcome in childhood medulloblastoma: the United Kingdom Children's Cancer Study Group Brain Tumour Committee. J Clin Oncol 23:7951–7957

Fattet S, Haberler C, Legoix P, Varlet P, Lellouch-Tubiana A, Lair S, Manie E, Raquin MA, Bours D, Carpentier S, Barillot E, Grill J, Doz F, Puget S, Janoueix-Lerosey I, Delattre O (2009) Beta-catenin status in paediatric medulloblastomas: correlation of immunohistochemical expression with mutational status, genetic profiles, and clinical characteristics. J Pathol 218:86–94

Feng Y, Tian ZM, Wan MX, Zheng ZB (2007) Protein profile of human hepatocarcinoma cell line SMMC-7721: identification and functional analysis. World J Gastroenterol 13:2608–2614

Giampietro C, Luzzati F, Gambarotta G, Giacobini P, Boda E, Fasolo A, Perroteau I (2005) Stathmin expression modulates migratory properties of GN-11 neurons in vitro. Endocrinology 146:1825–1834

Gilbertson R, Wickramasinghe C, Hernan R, Balaji V, Hunt D, Jones-Wallace D, Crolla J, Perry R, Lunec J, Pearson A, Ellison D (2001) Clinical and molecular stratification of disease risk in medulloblastoma. Br J Cancer 85:705–712

Goldwein JW, Radcliffe J, Johnson J, Moshang T, Packer RJ, Sutton LN, Rorke LB, D'Angio GJ (1996) Updated results of a pilot study of low dose craniospinal irradiation plus chemotherapy for children under five with cerebellar primitive neuroectodermal tumors (medulloblastoma). Int J Radiat Oncol Biol Phys 34:899–904

Grotzer MA, Hogarty MD, Janss AJ, Liu X, Zhao H, Eggert A, Sutton LN, Rorke LB, Brodeur GM, Phillips PC (2001) MYC messenger RNA expression predicts survival outcome in childhood primitive neuroectodermal tumor/medulloblastoma. Clin Cancer Res 7:2425–2433

Grotzer MA, von Hoff K, von Bueren AO, Shalaby T, Hartmann W, Warmuth-Metz M, Emser A, Kortmann RD, Kuehl J, Pietsch T, Rutkowski S (2007) Which clinical and biological tumor markers proved predictive in the prospective multicenter trial HIT'91—implications for investigating childhood medulloblastoma. Klin Padiatr 219:312–317

Gruber-Olipitz M, Strobel T, Kang SU, John JP, Grotzer MA, Slavc I, Lubec G (2009) Neurotrophin 3/TrkC-regulated proteins in the human medulloblastoma cell line DAOY. Electrophoresis 30:540–549

Hait WN, Yang JM (2006) The individualization of cancer therapy: the unexpected role of p53. Trans Am Clin Climatol Assoc 117:85–101 (discussion 101)

Haley B, Paunesku T, Protic M, Woloschak GE (2009) Response of heterogeneous ribonuclear proteins (hnRNP) to ionising radiation and their involvement in DNA damage repair. Int J Radiat Biol 85:643–655

Hamilton SR, Liu B, Parsons RE, Papadopoulos N, Jen J, Powell SM, Krush AJ, Berk T, Cohen Z, Tetu B et al (1995) The molecular basis of Turcot's syndrome. N Engl J Med 332:839–847

Harris MN, Ozpolat B, Abdi F, Gu S, Legler A, Mawuenyega KG, Tirado-Gomez M, Lopez-Berestein G, Chen X (2004) Comparative proteomic analysis of all-*trans*-retinoic acid treatment reveals systematic posttranscriptional control mechanisms in acute promyelocytic leukemia. Blood 104:1314–1323

He TC, Sparks AB, Rago C, Hermeking H, Zawel L, da Costa LT, Morin PJ, Vogelstein B, Kinzler KW (1998) Identification of c-MYC as a target of the APC pathway. Science 281:1509–1512

Henriksson M, Luscher B (1996) Proteins of the Myc network: essential regulators of cell growth and differentiation. Adv Cancer Res 68:109–182

Heo S, Lubec G (2010) Generation and characterization of a specific polyclonal antibody against the mouse serotonin receptor 1A: a state-of-the-art recommendation on how to characterize antibody specificity. Electrophoresis 31:3789–3796

Herms J, Neidt I, Luscher B, Sommer A, Schurmann P, Schroder T, Bergmann M, Wilken B, Probst-Cousin S, Hernaiz-Driever P, Behnke J, Hanefeld F, Pietsch T, Kretzschmar HA (2000) C-MYC expression in medulloblastoma and its prognostic value. Int J Cancer 89:395–402

Hossain MN, Fuji M, Miki K, Endoh M, Ayusawa D (2007) Downregulation of hnRNP C1/C2 by siRNA sensitizes HeLa cells to various stresses. Mol Cell Biochem 296:151–157

Ide T, Brown-Endres L, Chu K, Ongusaha PP, Ohtsuka T, El-Deiry WS, Aaronson SA, Lee SW (2009) GAMT, a p53-inducible modulator of apoptosis, is critical for the adaptive response to nutrient stress. Mol Cell 36:379–392

Jemal A, Siegel R, Ward E, Hao Y, Xu J, Murray T, Thun MJ (2008) Cancer statistics, 2008. CA Cancer J Clin 58:71–96

Jin K, Mao XO, Cottrell B, Schilling B, Xie L, Row RH, Sun Y, Peel A, Childs J, Gendeh G, Gibson BW, Greenberg DA (2004) Proteomic and immunochemical characterization of a role for stathmin in adult neurogenesis. Faseb J 18:287–299

Kim JH, Paek KY, Choi K, Kim TD, Hahm B, Kim KT, Jang SK (2003) Heterogeneous nuclear ribonucleoprotein C modulates translation of c-myc mRNA in a cell cycle phase-dependent manner. Mol Cell Biol 23:708–720

Kokkinakis DM, Liu X, Chada S, Ahmed MM, Shareef MM, Singha UK, Yang S, Luo J (2004) Modulation of gene expression in human central nervous system tumors under methionine deprivation-induced stress. Cancer Res 64:7513–7525

Korshunov A, Benner A, Remke M, Lichter P, von Deimling A, Pfister S (2008) Accumulation of genomic aberrations during clinical progression of medulloblastoma. Acta Neuropathol 116:383–390

Kouzu Y, Uzawa K, Koike H, Saito K, Nakashima D, Higo M, Endo Y, Kasamatsu A, Shiiba M, Bukawa H, Yokoe H, Tanzawa H (2006) Overexpression of stathmin in oral squamous-cell carcinoma: correlation with tumour progression and poor prognosis. Br J Cancer 94:717–723

Kuo MF, Wang HS, Kuo QT, Shun CT, Hsu HC, Yang SH, Yuan RH (2009) High expression of stathmin protein predicts a fulminant course in medulloblastoma. J Neurosurg Pediatr 4:74–80

Liu J, Levens D (2006) Making myc. Curr Top Microbiol Immunol 302:1–32

MacDonald TJ, Rood BR, Santi MR, Vezina G, Bingaman K, Cogen PH, Packer RJ (2003) Advances in the diagnosis, molecular genetics, and treatment of pediatric embryonal CNS tumors. Oncologist 8:174–186

MacLeod JC, Sayer RJ, Lucocq JM, Hubbard MJ (2004) ERp29, a general endoplasmic reticulum marker, is highly expressed throughout the brain. J Comp Neurol 477:29–42

Meffert G, Gellerich FN, Margreiter R, Wyss M (2005) Elevated creatine kinase activity in primary hepatocellular carcinoma. BMC Gastroenterol 5:9

Melhem RF, Zhu XX, Hailat N, Strahler JR, Hanash SM (1991) Characterization of the gene for a proliferation-related phosphoprotein (oncoprotein 18) expressed in high amounts in acute leukemia. J Biol Chem 266:17747–17753

Mistry SJ, Bank A, Atweh GF (2007) Synergistic antiangiogenic effects of stathmin inhibition and taxol exposure. Mol Cancer Res 5:773–782

Mkrtchian S, Baryshev M, Sargsyan E, Chatzistamou I, Volakaki AA, Chaviaras N, Pafiti A, Triantafyllou A, Kiaris H (2008) ERp29, an endoplasmic reticulum secretion factor is involved in the growth of breast tumor xenografts. Mol Carcinog 47:886–892

Mori T, Nagase H, Horii A, Miyoshi Y, Shimano T, Nakatsuru S, Aoki T, Arakawa H, Yanagisawa A, Ushio Y et al (1994) Germline and somatic mutations of the APC gene in patients with Turcot syndrome and analysis of APC mutations in brain tumors. Genes Chromosomes Cancer 9:168–172

Neben K, Korshunov A, Benner A, Wrobel G, Hahn M, Kokocinski F, Golanov A, Joos S, Lichter P (2004) Microarray-based screening for molecular markers in medulloblastoma revealed STK15 as independent predictor for survival. Cancer Res 64:3103–3111

Nesbit CE, Tersak JM, Prochownik EV (1999) MYC oncogenes and human neoplastic disease. Oncogene 18:3004–3016

Ngo TT, Peng T, Liang XJ, Akeju O, Pastorino S, Zhang W, Kotliarov Y, Zenklusen JC, Fine HA, Maric D, Wen PY, De Girolami U, Black PM, Wu WW, Shen RF, Jeffries NO, Kang DW, Park JK (2007) The 1p-encoded protein stathmin and resistance of malignant gliomas to nitrosoureas. J Natl Cancer Inst 99:639–652

Obaya AJ, Mateyak MK, Sedivy JM (1999) Mysterious liaisons: the relationship between c-Myc and the cell cycle. Oncogene 18:2934–2941

Packer RJ (2008) Childhood brain tumors: accomplishments and ongoing challenges. J Child Neurol 23:1122–1127

Pfister S, Remke M, Benner A, Mendrzyk F, Toedt G, Felsberg J, Wittmann A, Devens F, Gerber NU, Joos S, Kulozik A, Reifenberger G, Rutkowski S, Wiestler OD, Radlwimmer B, Scheurlen W, Lichter P, Korshunov A (2009) Outcome prediction in pediatric medulloblastoma based on DNA copy-number aberrations of chromosomes 6q and 17q and the MYC and MYCN loci. J Clin Oncol 27:1627–1636

Prendergast GC (1999) Mechanisms of apoptosis by c-Myc. Oncogene 18:2967–2987

Radcliffe J, Packer RJ, Atkins TE, Bunin GR, Schut L, Goldwein JW, Sutton LN (1992) Three- and four-year cognitive outcome in children with noncortical brain tumors treated with whole-brain radiotherapy. Ann Neurol 32:551–554

Ray A, Ho M, Ma J, Parkes RK, Mainprize TG, Ueda S, McLaughlin J, Bouffet E, Rutka JT, Hawkins CE (2004) A clinicobiological model predicting survival in medulloblastoma. Clin Cancer Res 10:7613–7620

Rogers HA, Miller S, Lowe J, Brundler MA, Coyle B, Grundy RG (2009) An investigation of WNT pathway activation and association with survival in central nervous system primitive neuroectodermal tumours (CNS PNET). Br J Cancer 100:1292–1302

Rubin CI, Atweh GF (2004) The role of stathmin in the regulation of the cell cycle. J Cell Biochem 93:242–250

Rutkowski S, von Bueren A, von Hoff K, Hartmann W, Shalaby T, Deinlein F, Warmuth-Metz M, Soerensen N, Emser A, Bode U, Mittler U, Urban C, Benesch M, Kortmann RD, Schlegel PG, Kuehl J, Pietsch T, Grotzer M (2007) Prognostic relevance of clinical and biological risk factors in childhood medulloblastoma: results of patients treated in the prospective multicenter trial HIT'91. Clin Cancer Res 13:2651–2657

Rutkowski S, Gerber NU, von Hoff K, Gnekow A, Bode U, Graf N, Berthold F, Henze G, Wolff JE, Warmuth-Metz M, Soerensen N, Emser A, Ottensmeier H, Deinlein F, Schlegel PG, Kortmann RD, Pietsch T, Kuehl J (2009) Treatment of early childhood medulloblastoma by postoperative chemotherapy and deferred radiotherapy. Neuro Oncol 11:201–210

Sargsyan E, Baryshev M, Szekely L, Sharipo A, Mkrtchian S (2002) Identification of ERp29, an endoplasmic reticulum lumenal protein, as a new member of the thyroglobulin folding complex. J Biol Chem 277:17009–17015

Scheurlen WG, Schwabe GC, Joos S, Mollenhauer J, Sorensen N, Kuhl J (1998) Molecular analysis of childhood primitive neuroectodermal tumors defines markers associated with poor outcome. J Clin Oncol 16:2478–2485

Schmidt EV (1999) The role of c-myc in cellular growth control. Oncogene 18:2988–2996

Silber JH, Radcliffe J, Peckham V, Perilongo G, Kishnani P, Fridman M, Goldwein JW, Meadows AT (1992) Whole-brain irradiation and decline in intelligence: the influence of dose and age on IQ score. J Clin Oncol 10:1390–1396

Siu IM, Lal A, Blankenship JR, Aldosari N, Riggins GJ (2003) c-Myc promoter activation in medulloblastoma. Cancer Res 63:4773–4776

Spahn A, Blondeau N, Heurteaux C, Dehghani F, Rami A (2008) Concomitant transitory up-regulation of X-linked inhibitor of apoptosis protein (XIAP) and the heterogeneous nuclear ribonucleoprotein C1–C2 in surviving cells during neuronal apoptosis. Neurochem Res 33:1859–1868

Stearns D, Chaudhry A, Abel TW, Burger PC, Dang CV, Eberhart CG (2006) c-myc overexpression causes anaplasia in medulloblastoma. Cancer Res 66:673–681

Stockler S, Schutz PW, Salomons GS (2007) Cerebral creatine deficiency syndromes: clinical aspects, treatment and pathophysiology. Subcell Biochem 46:149–166

Sun W, Xing B, Sun Y, Du X, Lu M, Hao C, Lu Z, Mi W, Wu S, Wei H, Gao X, Zhu Y, Jiang Y, Qian X, He F (2007) Proteome analysis of hepatocellular carcinoma by two-dimensional difference gel electrophoresis: novel protein markers in hepatocellular carcinoma tissues. Mol Cell Proteomics 6:1798–1808

Takahashi M, Yang XJ, Lavery TT, Furge KA, Williams BO, Tretiakova M, Montag A, Vogelzang NJ, Re GG, Garvin AJ, Soderhall S, Kagawa S, Hazel-Martin D, Nordenskjold A, Teh BT (2002) Gene expression profiling of favorable histology Wilms tumors and its correlation with clinical features. Cancer Res 62:6598–6605

von Bueren AO, Shalaby T, Rajtarova J, Stearns D, Eberhart CG, Helson L, Arcaro A, Grotzer MA (2007) Anti-proliferative activity of the quassinoid NBT-272 in childhood medulloblastoma cells. BMC Cancer 7:19

von Bueren AO, Shalaby T, Oehler-Janne C, Arnold L, Stearns D, Eberhart CG, Arcaro A, Pruschy M, Grotzer MA (2009) RNA interference-mediated c-MYC inhibition prevents cell growth and decreases sensitivity to radio- and chemotherapy in childhood medulloblastoma cells. BMC Cancer 9:10

von Hoff K, Hinkes B, Gerber NU, Deinlein F, Mittler U, Urban C, Benesch M, Warmuth-Metz M, Soerensen N, Zwiener I, Goette H, Schlegel PG, Pietsch T, Kortmann RD, Kuehl J, Rutkowski S (2009) Long-term outcome and clinical prognostic factors in children with medulloblastoma treated in the prospective randomised multicentre trial HIT'91. Eur J Cancer 45:1209–1217

von Hoff K, Hartmann W, von Bueren AO, Gerber NU, Grotzer MA, Pietsch T, Rutkowski S (2010) Large cell/anaplastic medulloblastoma: outcome according to myc status, histopathological, and clinical risk factors. Pediatr Blood Cancer 54:369–376

Wei SH, Lin F, Wang X, Gao P, Zhang HZ (2008) Prognostic significance of stathmin expression in correlation with metastasis and clinicopathological characteristics in human ovarian carcinoma. Acta Histochem 110:59–65

Yuan RH, Jeng YM, Chen HL, Lai PL, Pan HW, Hsieh FJ, Lin CY, Lee PH, Hsu HC (2006) Stathmin overexpression cooperates with p53 mutation and osteopontin overexpression, and is associated with tumour progression, early recurrence, and poor prognosis in hepatocellular carcinoma. J Pathol 209:549–558

Zeltzer PM, Boyett JM, Finlay JL, Albright AL, Rorke LB, Milstein JM, Allen JC, Stevens KR, Stanley P, Li H, Wisoff JH, Geyer JR, McGuire-Cullen P, Stehbens JA, Shurin SB, Packer RJ (1999) Metastasis stage, adjuvant treatment, and residual tumor are prognostic factors for medulloblastoma in children: conclusions from the Children's Cancer Group 921 randomized phase III study. J Clin Oncol 17:832–845

Zurawel RH, Chiappa SA, Allen C, Raffel C (1998) Sporadic medulloblastomas contain oncogenic beta-catenin mutations. Cancer Res 58:896–899